

COVER PAGE

Document downloaded by @DAEL

Mon Nov 9 07:58:52 2026
For personal use

When automatic English translation is provided, only the original document is authentic.
The EAA cannot be held responsible of any translation error

Bibliographical reference

Acoustic Meta-materials Incorporating the KDamper Concept for Low Frequency Acoustic Isolation, Ioannis A. Antoniadis and Andreas Paradeisiotis, Acta Acustica **vol. 104** (Number 4), 2018, pp. 636-646

DOI
https://doi.org/10.3813/AAA.919203

Acta Acustica united with Acustica
Vol. 104 (2018) 636 – 646

DOI 10.3813/AAA.919203

Acoustic Meta-materials Incorporating the KDamper Concept for Low Frequency Acoustic Isolation

Ioannis A. Antoniadis, Andreas Paradeisiotis
Dynamics and Structures, Mechanical Engineering, NTUA, Athens, 15780 Zografou, Greece.
antogian@central.ntua.gr

Summary
Periodic structures with unit cells exhibiting local resonance known as "acoustic/elastic meta-materials", present unique wave propagation properties at wavelengths well below the regime corresponding to band-gap generation based on spatial periodicity. Therefore, they are rendered especially suitable in low-frequency range applications. In order to overcome the main constraints encountered in such cases, including heavy internal oscillating masses with amplitude limitations, the KDamping passive, vibration isolation and damping concept is proposed as the base of the periodic structure. According to this concept, the resulting acoustic/elastic meta-materials are designed to include negative stiffness elements instead of or in addition to the internally resonating masses. This, deals effectively with the requirement for heavy locally added masses, while simultaneously exploits the negative stiffness damping phenomenon. Analysis of the one-dimensional mass-in-mass lattice via application of Bloch's theory and classical modal analysis is performed and the corresponding dispersion relations are derived. Furthermore, a preliminary examination of a practical implementation is attempted via structural realization of the aforementioned negative stiffness element. Additionally, the KDamper meta-material is analysed and subjected to harmonic and broadband noise excitations. Corresponding results and comparisons between the KDamper, "m-k-m" (mass-spring-mass) and Tuned Mass Damper based periodic structures, indicate significant improvements and advantages over the conventional mass-in-mass lattice, such as broader band-gaps and increased damping ratio, revealing significant potential in low frequency acoustic isolation/damping.

PACS no. 43.20.-f, 43.40.-r

1. Introduction

The terms "acoustic/elastic meta-materials" [1] describe a class of periodic structures with unit cells exhibiting local resonance. An intuitive description of such designs lies in use of a simple "mass-in-mass" lumped parameter model, resulting in negative effective stiffness and/or mass at frequency ranges close to the local resonances. Unlike phononic crystals [2, 3], which are based on Bragg scattering, this localized resonant structure has been shown [4, 5, 6, 7] to exhibit band-gaps at wavelengths much longer than the lattice size, thus enabling low-frequency vibration attenuation, wave guiding, and filtering, among other applications. Preliminary applications include among others vibration absorption in beams [8, 9] and plates [10, 11].

However, low frequency range applications of such locally resonant meta-materials, may require very heavy internal moving masses, as well as additional constraints at the amplitudes of the internally oscillating locally resonating structures, which may prohibit their practical implementation. For example, current applications of locally resonant meta-materials in acoustics [12, 13] often address frequencies well above 500 [Hz]. However, there are some notable applications in low frequency noise isolation based on thin membrane-type acoustic meta-materials, serving as a total reflection nodal surface at certain frequencies [14]. Another example is the sound absorption and reflection from a resonant meta-surface [15], achieving total sound absorption at resonance observed in an impedance tube, below 400 Hz. However, it should be mentioned, that in this frequency range, the performance of conventional noise insulation materials is quite poor.

To contribute to the solution of low frequency sound attenuation, the paper considers the application of the KDamping concept towards the design of highly dissipative low-frequency elastic/ acoustic meta-materials. The KDamper [16] is a novel passive vibration isolation and damping concept, based essentially on the optimal combination of appropriate stiffness elements, which include a negative stiffness element. The KDamper can be considered as an extension of the traditional Tuned Mass Damper (TMD), by the addition of a negative stiffness element to the internal oscillating mass. This idea was first sug-

Received 25 July 2017,
accepted 22 May 2018.

© S. Hirzel Verlag · EAA

Document downloaded by @DAEL, 2026-11-09 07:58:54 - personal use only

gested in [16] and was further treated in a systematic way in [17], within the context of the design of a general class of tuned mass dampers. A preliminary review of the reported physical principles for the design of negative stiffness elements can be found in [17]. These principles include conventional pre-stressed elastic mechanical elements, such as post-buckled beams, plates, shells and pre-compressed springs arranged in appropriate geometrical configurations, or other sources of forces, such as gravitational, magnetic or electromagnetic.

Contrary to the TMD and its variants, the KDamper substitutes the inertial forces of the added TMD mass by the stiffness force of the negative stiffness element. Among others, this can provide significant comparative advantages, especially in the very low frequency range. As a result, the KDamper can achieve better damping characteristics, without the need of additional heavy masses, as in the case of the TMD. Moreover, since the isolation and damping properties of the KDamper essentially result from the stiffness elements of the system, further technological advantages can emerge, in terms of weight, complexity and reliability.

Based on the periodic repetition of KDamper elements, a novel class of meta-materials can be designed, in the same way that the periodic repetition of TMDs consists the conceptual framework under which the locally resonant meta-materials in [16] are analysed. Preliminary results [18, 19] confirm the efficiency of this approach. Towards this direction, it should be noted that recently, numerous periodic cellular structures with advanced dynamic behaviour have been also proposed, [20, 21, 22, 23] combining high positive and negative stiffness elements, such as buckled beams or chiral structures.

Application of both Bloch's theory (Subsec. 2.2) and the classical modal analysis (Sect. 2.3) for the one-dimensional mass-in-mass lattice is analysed and the corresponding dispersion relations are derived. The results (Sect. 3) indicate significant advantages over the conventional mass-in-a mass lattice, such as broader band-gaps and increased damping ratio and reveal significant potential in the proposed solution. A preliminary feasibility analysis (Sect. 3) for low frequency acoustic isolation-damping confirms the strong potential and applicability of this concept.

2. KDamper Meta-materials

2.1. Overview of the KDamper Concept

Figure 1 presents the basic layout of the KDamper concept [17], which is designed to minimize the response $u_S(t)$ of an undamped SDoF system of mass m and static stiffness k_0 to an external excitation $f(t)$.

In order to overcome limitations regarding the static loading capacity of the structure –which may result in unsolvable problems (e.g. collapse of structure), especially for vertical vibration isolation– the KDamper uses a negative stiffness element k_N along with the basic requirement

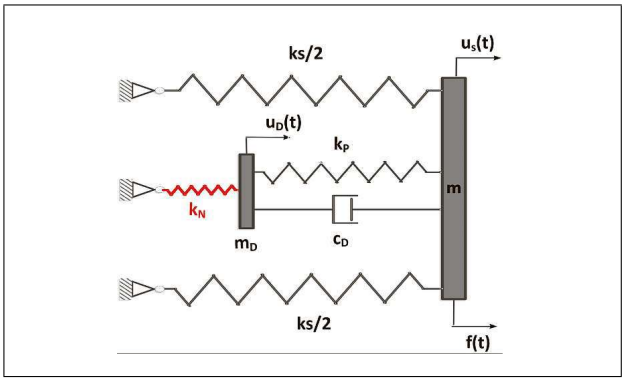


Figure 1. KDamper vibration absorption concept.

that the overall static stiffness k_0 of the system is maintained as

$$k_0 = \frac{k_P k_N}{k_P + k_N} + k_S \tag{1}$$

and the natural frequency comes as

$$\omega_0 = \sqrt{k_0/m}. \tag{2}$$

Compared to the conventional TMD, the additional negative stiffness element k_N, is inserted between the additional mass and the ground. Thus, the equation of motion of the KDamper becomes

$$m\ddot{u}_S + c_D(\dot{u}_S - \dot{u}_D) + k_S u_S + k_P(u_S - u_D) = f(t), \tag{3}$$
$$m_D\ddot{u}_D - c_D(\dot{u}_S - \dot{u}_D) + k_N u_D - k_P(u_S - u_D) = 0. \tag{4}$$

Assuming a harmonic excitation in the form of

$$f(t) = \tilde{F}\, e^{J\omega t} \tag{5}$$

and a steady state complex response of

$$u_S(t) = \tilde{U}_S e^{J\omega t}, \tag{6}$$
$$u_D(t) = \tilde{U}_D e^{J\omega t}, \tag{7}$$

the equations of motion of the KDamper can be expressed as

$$-\omega^2 m\tilde{U}_S + k_S\tilde{U}_S - \omega^2 m_D\tilde{U}_D + k_N\tilde{U}_D = \tilde{F}, \tag{8}$$
$$-\omega^2 m_D\tilde{U}_D - J\omega c_D(\tilde{U}_S - \tilde{U}_D) - k_P(\tilde{U}_S - \tilde{U}_D) + k_N\tilde{U}_D = 0. \tag{9}$$

Examination of Equation (8) reveals that the amplitude F_{MD} of the inertia force of the additional mass m_D and the amplitude F_N of the negative stiffness force are exactly in phase, due to the negative value of k_N.

$$F_{MD} = -\omega^2 m_D\tilde{U}_D, \tag{10}$$
$$F_N = k_N\tilde{U}_D \le 0. \tag{11}$$

Thus, the KDamper presents an indirect way of increasing the inertia effect of the additional mass m_D without however increasing directly the mass m_D itself. Moreover,

Document downloaded by @DAEL, 2026-11-09 07:58:54 - personal use only

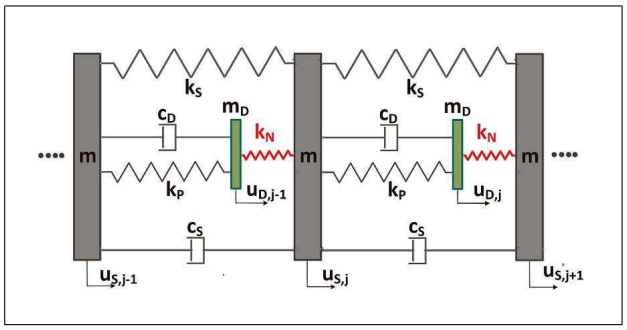


Figure 2. Unit cell of KDamper meta-material.

it should be noted that the value of $-\omega^2 m_D$, see Equation (10), depends on the frequency, while the value of k_N, see Equation (11), is constant in the entire frequency range, a fact which is of particular importance in low frequency vibration isolation.

The basic parameters of the KDamper concept [15] are μ,κ and ρ, which are defined as

$$\mu = m_D/m, \tag{12}$$
$$\rho = \omega_D/\omega_0, \tag{13}$$
$$\kappa = -\frac{k_N}{k_N + k_P}, \tag{14}$$

where $\omega_D = \sqrt{(k_P + k_N)/m_D}$. The optimal value of ρ where the transfer function of the displacement u_S (Figure 1) with regard to the excitation is minimized at a selected frequency, is defined as

$$\rho_{opt} = \sqrt{\frac{1}{(1+\mu+\kappa\mu)(1+\mu) - \kappa^2\mu}} \tag{15}$$

in terms of the parameters μ and κ. By setting the denominator of ρ_{opt} equal to zero, the maximum value that can be reached for κ is determined as

$$\kappa_{\max} = \frac{(1+\mu)(1+\sqrt{1+4/\mu})}{2}. \tag{16}$$

Therefore the value of κ can be selected as a fraction of $\kappa_{\max}$, namely

$$\kappa = (0:1)\cdot\kappa_{\max}. \tag{17}$$

As explained in detail in [17], the oscillator presents better vibration absorption capabilities when $\kappa \to \kappa_{\max}$ but at the same time needs to be considered that for $\kappa \to \kappa_{\max}$, the static stability margin of the oscillator tends to be nullified, because the overall static stiffness k_0 of the system in Equation (1) becomes negative.

2.2. Bloch analysis

The KDamper based meta-materials essentially comprise a periodic repetition of unit lattice cells of KDamper elements, as presented in Figure 2.

As evident from Figure 2, setting the value of the negative stiffness element of the KDamper unit cell as $k_N = 0$, makes it equivalent to the TMD based, acoustic/elastic locally resonant meta-materials. In view of Figure 2, the equations of motion of a typical unit cell become

$$\begin{aligned} m\ddot{u}_{S,j} + c_S(\dot{u}_{S,j} - \dot{u}_{S,j-1}) + c_S(\dot{u}_{S,j} - \dot{u}_{S,j+1}) \\ +k_S(u_{S,j} - u_{S,j-1}) + k_S(u_{S,j} - u_{S,j+1}) \\ +k_P(u_{S,j} - u_{D,j}) + k_N(u_{S,j} - u_{D,j-1}) = 0, \end{aligned} \tag{18}$$

$$\begin{aligned} m\ddot{u}_{D,j} + c_D(\dot{u}_{D,j} - \dot{u}_{S,j}) + k_P(u_{D,j} - u_{S,j}) \\ +k_N(u_{D,j} - u_{S,j+1}) = 0. \end{aligned} \tag{19}$$

2.2.1. Application of Bloch's theorem

For each of the system of Equations (18) and (19), the generalized form [24] of Bloch's theorem is applied

$$u_{S,j} = U_S\, e^{\lambda t} \tag{20}$$
$$u_{S,j+1} = U_S\, e^{jkl+\lambda t} = U_{S,j+1}\, e^{\lambda t} \tag{21}$$
$$u_{S,j-1} = U_S\, e^{-jkl+\lambda t} = U_{S,j-1}\, e^{\lambda t} \tag{22}$$

$$u_{D,j} = U_D\, e^{\lambda t} \tag{23}$$
$$u_{D,j+1} = U_D\, e^{jkl+\lambda t} = U_{D,j+1}\, e^{\lambda t} \tag{24}$$
$$u_{D,j-1} = U_D\, e^{-jkl+\lambda t} = U_{D,j-1}\, e^{\lambda t} \tag{25}$$

where U_S, U_D are the wave amplitudes at node j, l is the unit-cell length, k is the wave number and λ is a complex frequency function that permits wave attenuation in time. In the limiting case of no damping, $\lambda = j\omega$, and the usual form of Bloch's theorem is recovered. Substitution of Equations (20)-(22) and (23)–(25) into Equations (18)–(19), leads to

$$\begin{aligned} \left[\lambda^2 m + \lambda(\gamma c_S + c_D) + (\gamma k_S + k_P + k_N)\right]U_S \\ -(\lambda c_D + k_P + e^{jkl}k_N)U_D = 0, \end{aligned} \tag{26}$$

$$\begin{aligned} \left[\lambda^2 m_D + \lambda c_D + (k_P + k_N)\right]U_D \\ -(\lambda c_D + k_P + e^{-jkl}k_N)U_S = 0, \end{aligned} \tag{27}$$

where

$$\begin{aligned} \gamma &= 2 - (e^{jkl} + e^{-jkl}) \\ &= 2(1 - \cos kl) = 2(1 - \cos q), \end{aligned} \tag{28}$$
$$q = kl. \tag{29}$$

Substituting U_D from Equation (27) into Equation (26), leads to

$$\left[\alpha_4\lambda^4 + \alpha_3\lambda^3 + \alpha_2\lambda^2 + \alpha_1\lambda + \alpha_0\right]U_S = 0, \tag{30}$$

where

$$\alpha_4 = m_D m, \tag{31}$$
$$\alpha_3 = (m_D + m)c_D + \gamma c_S m_D, \tag{32}$$
$$\alpha_2 = (m_D + m)(k_P + k_N) + \gamma(c_S c_D + k_S m_D,) \tag{33}$$
$$\alpha_1 = \gamma c_S(k_P + k_N) + \gamma c_D(k_S + k_N), \tag{34}$$
$$\alpha_0 = \gamma k_S(k_P + k_N) + \gamma k_P k_N. \tag{35}$$

Document downloaded by @DAEL, 2026-11-09 07:58:54 - personal use only

2.2.2. Bandgap estimation and properties

Equation (30) yields a characteristic equation of the form

$$\alpha_4\lambda^4 + \alpha_3\lambda^3 + \alpha_2\lambda^2 + \alpha_1\lambda + \alpha_0 = 0. \tag{36}$$

The roots obtained from Equation (36) may be expressed as

$$\lambda_B = -\zeta_B(k)\omega_B \pm j\omega_B\sqrt{1-\zeta_B^2(k)}, \quad B = 1, 2, \tag{37}$$

where $B = 1$ represents the lower branch number and $B = 2$ represents the upper branch number of the two dispersion curves and ω_B, ζ_B represent their corresponding natural frequency and damping ratio. Assuming an undamped system, the following are defined ($\alpha_3 = \alpha_1 = 0$, $\lambda_B = \pm j\omega_B$):

$$\alpha_4 = m_D m, \tag{38}$$
$$\alpha_2 = (m_D + m)k_I + \gamma\, k_S m_D = \alpha_{2,0} + \gamma\,\alpha_{2,\gamma}, \tag{39}$$
$$\alpha_0 = \gamma[k_S(k_P + k_N) + k_P k_N] = \gamma\alpha_{0,\gamma}, \tag{40}$$
$$k_I = k_P + k_N. \tag{41}$$

The bandgap limits can be obtained from Equation (42)

$$\alpha_4\omega^4 - (\alpha_{2,0} + \gamma\alpha_{2,\gamma})\omega^2 + \gamma\alpha_{0,\gamma} = 0, \tag{42}$$

which leads to:

$$\gamma = \omega^2\frac{\alpha_{2,0} - \alpha_4\omega^2}{\alpha_{0,\gamma} - \alpha_{2,\gamma}\omega^2}. \tag{43}$$

Therefore

$$\cos q = 1 - \frac{\omega^2}{2}\frac{\omega_H^2\omega_I^2 - \omega^2}{\omega_0^2\omega_I^2 - \omega_S^2\omega^2}, \tag{44}$$

where

$$\omega_I = \sqrt{k_I/m_D}, \tag{45}$$
$$\omega_H = \omega_I\sqrt{1+\mu}, \tag{46}$$
$$\omega_S = \sqrt{(k_S/m)}. \tag{47}$$

In view of the denominator and numerator of Equation (44), the band gap limits are [25]

$$\omega_L \le \omega \le \omega_H, \tag{48}$$

where

$$\omega_L^2 = \frac{\omega_0^2}{\frac{1}{\rho^2} + \kappa(1+\kappa)\mu} = \frac{\omega_I^2}{1 + \kappa(1+\kappa)\mu\rho^2}, \tag{49}$$
$$b_W = \frac{\omega_H - \omega_L}{\omega_L}$$
$$= \sqrt{(1+\mu)\left[1 + \kappa(1+\kappa)\mu\rho^2\right]} - 1, \tag{50}$$
$$\rho = \omega_I/\omega_0. \tag{51}$$

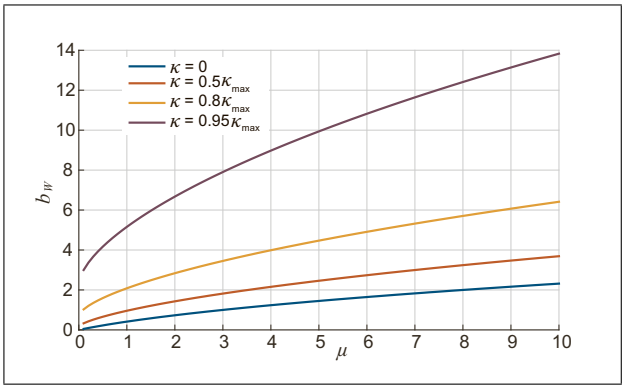


Figure 3. (Colour online) Normalized band-gap width as a function of the κ and μ KDamper parameters.

By setting $\kappa = 0$, the corresponding band-gap limits of the unit cell are obtained from Equations (49)-(51) as

$$\omega_L \xrightarrow{\kappa\to 0} \omega_I = \omega_D = \sqrt{k_P/m_D}, \tag{52}$$

$$b_W \xrightarrow{\kappa\to 0} \sqrt{1+\mu} - 1. \tag{53}$$

Observation of Equations (49) and (50), shows that the normalized band gap width b_W can be increased not only by increasing the parameter μ (i.e., the value of the internally oscillating mass m_D), but also the value of the parameter κ (i.e., the magnitude of the negative stiffness element k_N according to Equation (12)). This can be considered among others as a consequence of Equation (11), since the usage of a negative stiffness element can be considered as an indirect approach to artificially increase the inertia of the system.

Figure 3 presents the resulting normalized band gap widths b_W for a simultaneous variation of both the κ and μ parameters of the KDamper meta-material. As it can be observed, a normalized band gap width of $b_W = 3$ may already be achieved for values of κ close to $\kappa_{\max}$, even for negligible values of the internal oscillating mass ($\mu \approx 0$) . Band-gaps of such a width may not be accomplished by conventional acoustic meta-materials, even for extremely high values of the internal oscillating mass ($\mu \ge 10$).

The value of ρ and consequently the value of κ, are determined according to the traditional KDamper design concept [17] from Equations (15)-(17).

2.3. Modal analysis

Classic modal analysis provides better insight into the dynamics of elastic/acoustic meta-materials as it relaxes the assumption of Bloch's analysis for a perfect spatial repetition and can be used as an independent validation of the results of Bloch's analysis. The harmonic response of the undamped system is considered, with Equations (18)–(19) leading to

$$-\omega^2 U_{S,j} + k_S(U_{S,j} - U_{S,j-1}) + k_S(U_{S,j} - U_{S,j+1}) \tag{54}$$
$$+k_P(U_{S,j} - U_{D,j}) + k_N(U_{S,j} - U_{D,j-1}) = 0,$$
$$-\omega^2 m_D U_{D,j} + k_P(U_{D,j} - U_{S,j}) \tag{55}$$
$$+k_N(U_{D,j} - U_{S,j+1}) = 0.$$

Document downloaded by @DAEL, 2026-11-09 07:58:54 - personal use only

Algebraic elaboration leads to the succession of the following equivalent equations:

$$-\omega^2 U_{S,j}+k_S(2U_{S,j}-U_{S,j-1}-U_{S,j+1})+(k_P+k_N)U_{S,j} - \left[\frac{k_P^2 U_{S,j}+k_P k_N U_{S,j+1}}{-\omega^2 m_D+k_P+k_N}+\frac{k_N^2 U_{S,j}+k_P k_N U_{S,j-1}}{-\omega^2 m_D+k_P+k_N}\right]=0, \quad (56)$$

$$-\omega^2\left[m+\frac{m_D(k_P+k_N)}{-\omega^2 m_D+k_P+k_N}\right]U_{S,j} +\left[k_S+\frac{k_P k_N}{-\omega^2 m_D+k_P+k_N}\right](2U_{S,j}-U_{S,j-1}-U_{S,j+1})=0, \quad (57)$$

$$-\omega^2 m_{\text{eff}} U_{S,j}+k_{\text{eff}}(2U_{S,j}-U_{S,j-1}-U_{S,j+1})=0, \quad (58)$$

where

$$m_{\text{eff}} = m+\frac{m_D(k_P+k_N)}{-\omega^2 m_D+k_P+k_N} = m\left[1+\frac{\mu\omega_I^2}{-\omega^2+\omega_I^2}\right]=m\frac{\omega_H^2-\omega^2}{\omega_I^2-\omega^2}, \quad (59)$$

$$k_{\text{eff}} = k_S\left[1+\frac{(k_0/k_S-1)k_I}{-\omega^2 m_D+k_I}\right] = k_S\left[1+\frac{(\omega_0/\omega_S-1)\omega_I}{-\omega^2+\omega_I}\right]=k_S\frac{\omega_L^2-\omega^2}{\omega_I^2-\omega^2}. \quad (60)$$

Assuming a periodic system without the KDamper elements ($k_P = k_N = c_D = m_D = 0$), Equation(20) can be written in the following compact matrix notation:

$$-\omega^2\mathbf{M}\mathbf{U}_S+\mathbf{K}_S\mathbf{U}_S=0. \quad (61)$$

Using ω_k and Φ_k, $(k = 1 : N)$ to denote the natural frequencies and the eigenvectors of the system (Equation (61)) respectively, and exploiting their orthogonality properties,

$$\Phi_i^T\mathbf{M}\Phi_k = 1, \quad (62)$$

$$\Phi_i^T\mathbf{K}_S\Phi_k = \omega_k^2. \quad (63)$$

The following modal transform is obtained,

$$\mathbf{U}_S=\sum_{k=1}^{N}\Phi_k\eta_k, \quad (64)$$

where η_k is the vector of time dependent generalized coordinates.

2.3.1. Bandgap estimation and properties

An alternative equivalent approach for band-gap estimation is proposed in [26], based on the modal analysis executed above. Application of Equations (62)-(64) to the system of Equations (54)–(55) leads to a set of decoupled equations,

$$-\omega^2(\omega_H^2-\omega^2)\eta_k-\omega_k^2(\omega_L^2-\omega^2)\eta_k=0, \quad (65)$$

which can be written in the following non-dimensional form:

$$\Omega_k^2(\Omega_L^2-\Omega^2)-\Omega^2(\Omega_H^2-\Omega^2)=0. \quad (66)$$

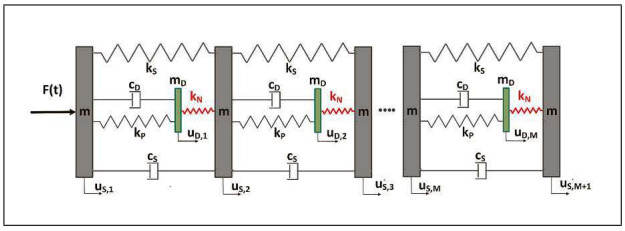


Figure 4. KDamper acoustic meta-material.

Therefore

$$\Omega^4-\Omega^2(\Omega_k^2+\Omega_H^2)+\Omega_k^2\Omega_L^2=0, \quad (67)$$

where

$$\Omega = \omega/\omega_I, \quad (68)$$

$$\Omega_k = \omega_k/\omega_I, \quad (69)$$

$$\Omega_L = \omega_L/\omega_I, \quad (70)$$

$$\Omega_H = \omega_H/\omega_I. \quad (71)$$

Equation (66) has two real roots,

$$\Omega_{MIN}^2 = \frac{\Omega_k^2+\Omega_H^2}{2}\left[1-\sqrt{1-\frac{4\Omega_k^2\Omega_L^2}{(\Omega_k^2+\Omega_H^2)^2}}\right], \quad (72)$$

$$\Omega_{MAX}^2 = \frac{\Omega_k^2+\Omega_H^2}{2}\left[1+\sqrt{1-\frac{4\Omega_k^2\Omega_L^2}{(\Omega_k^2+\Omega_H^2)^2}}\right]. \quad (73)$$

The band-gap limits $[\Omega_L,\Omega_H]$ of the system result [26] from Equations (72)–(73) as

$$\Omega_{MIN}^2 \xrightarrow{\Omega_k\to\infty} \Omega_L, \quad (74)$$

$$\Omega_{MAX}^2 \xrightarrow{\Omega_k\to\infty} \Omega_H. \quad (75)$$

3. Application for Acoustic Isolation

Although the KDamper concept can find multiple applications in low-frequency damping and absorption, an indicative concept for the implementation of KDamper based meta-materials towards the design of acoustic isolation-absorption panels is examined here.

3.1. Examination of KDamper Metamaterial

For a selected value of the frequency f_L,

$$\omega_L = 2\pi f_L, \quad (76)$$

and for a selected damping ratio ζ_D, the damping constant is calculated as

$$c_D = 2\zeta_D\sqrt{(k_P+k_N)m_D} = 2\zeta_D\omega_I m_D. \quad (77)$$

The values of ρ and κ, are determined from Equations (15)-(17) according to the selected parameter μ. Thus, from Equation (49), the natural frequency should be

$$\omega_0=\omega_L\sqrt{\frac{1}{\rho^2}+\kappa(1+\kappa)\mu}. \quad (78)$$

Document downloaded by @DAEL, 2026-11-09 07:58:54 - personal use only

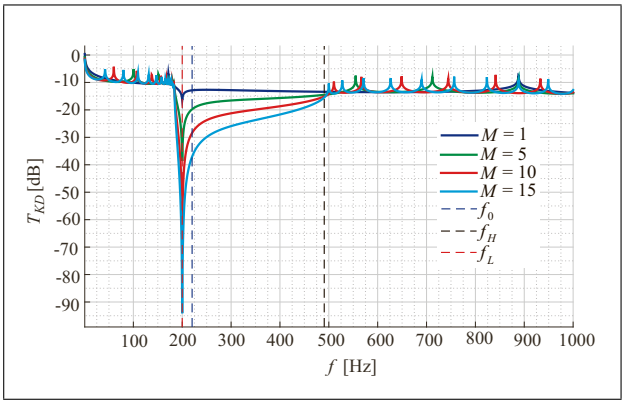


Figure 5. (Colour online) Comparison of KDamper meta-material transfer functions for increasing number of unit cells.

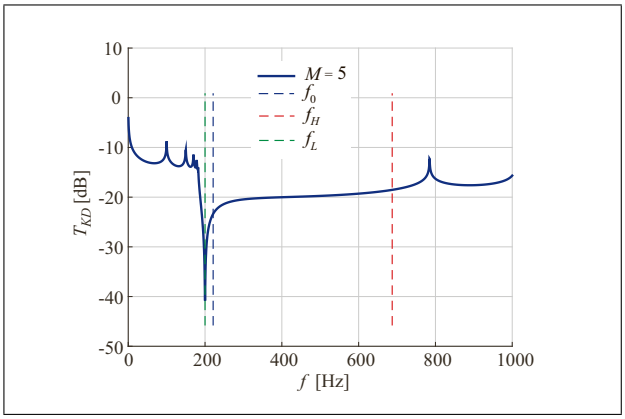


Figure 6. Transfer function of KDamper meta-material with M=5 number of unit cells.

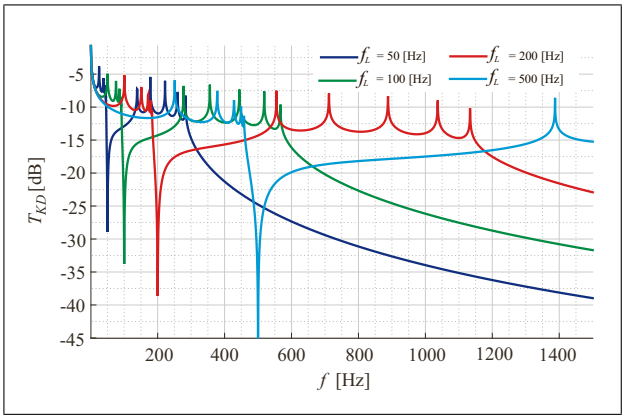


Figure 7. (Colour online) Transfer functions of KDamper meta-material with M=5 number of unit cells for various frequencies f_L.

Finally the values of ω_I, ω_H and b_w can be calculated according to Equations (2),(45) and (50). Consequently, the equation of motion of the meta-material, for M number of unit cells is expressed in matrix formulation as

$$\mathbf{M}\,\ddot{\mathbf{u}}(\mathbf{t}) + \mathbf{C}\,\dot{\mathbf{u}}(\mathbf{t}) + \mathbf{K}\,\mathbf{u}(\mathbf{t}) = \mathbf{F}\,\mathbf{f}(\mathbf{t}), \tag{79}$$

where $\mathbf{M}_{n\times n}$, $\mathbf{C}_{n\times n}$, $\mathbf{K}_{n\times n}\ddot{\mathbf{u}}_{n\times 1}$, $\dot{\mathbf{u}}_{n\times 1}$, $\mathbf{u}_{n\times 1}$, $\mathbf{F}_{n\times 1}$ and $n = 2M + 1$ is the number of degrees of freedom of the meta-material. For a single unit cell, M=1, the mass (**M**), damping (**C**) and stiffness (**K**) matrices are

$$\mathbf{M} = \begin{bmatrix} m & 0 & 0 \\ 0 & m_D & 0 \\ 0 & 0 & m \end{bmatrix}, \quad \mathbf{C} = \begin{bmatrix} c_s + c_D & -c_D & -c_s \\ -c_D & c_D & 0 \\ -c_s & 0 & c_s \end{bmatrix} \tag{80}$$

$$\mathbf{K} = \begin{bmatrix} k_S + k_P & -k_P & -k_S \\ -k_P & k_P + k_N & -k_N \\ -k_S & -k_N & k_S + k_N \end{bmatrix}, \quad \mathbf{F} = \begin{bmatrix} 1 \\ 0 \\ 0 \end{bmatrix}$$

For $M > 1$, the above matrices of the single unit cell, are added appropriately. Therefore, the transfer functions of each degree of freedom to the excitation may be calculated via the following expression,

$$\mathbf{TF} = (-\omega^2\mathbf{M} + \jmath\,\mathbf{C} + \mathbf{K})^{-1}\mathbf{F}, \tag{81}$$

where

$$\mathbf{TF}_{n\times 1} = \left\{ \frac{\tilde{U}_{S,1}}{\tilde{F}} \;\; \frac{\tilde{U}_{D,1}}{\tilde{F}} \;\; \frac{\tilde{U}_{S,2}}{\tilde{F}} \;\; \frac{\tilde{U}_{D,2}}{\tilde{F}} \;\; \dots \;\; \frac{\tilde{U}_{S,M+1}}{\tilde{F}} \right\}^T. \tag{82}$$

The transfer function of the KDamper is defined as $T_{KD} = \frac{\tilde{u}_{S,M+1}}{\tilde{F}}$, which is examined further in the next section.

Figure 5 shows a comparison between the transfer functions of the KDamper based meta-material for $M = 1, 5, 10$ and 15 number of unit cells for a selected low band-gap frequency $f_L = 200\ [Hz]$, damping ratios $\zeta = c_s/(2\omega_0 m) = 0.15$, $\zeta_D = 0.707$ and κ is taken as $0.9\kappa_{\max}$.

It is observed that this meta-material offers satisfactory band-gap depth, namely over 20 $[dB]$ attenuation inside the band-gap, even for as low as $M = 5$ number of unit cells. Thus, for further examination regarding the behaviour of the meta-material at various frequencies f_L, the number of unit cells is chosen as $M = 5$. The corresponding transfer function for $f_L = 200$ is presented in Figure 6.

Table I. Band-gap width for each f_L selection.

f_L [Hz]	50	100	200	500
$f_H - f_L$ [Hz]	73	145	290	726

The corresponding frequencies f_0,f_H and f_L are noted with dashed lines. In order to examine the effect of the low frequency choice f_L on the band-gap depth and width, Figure 7 is generated. In all cases the acoustic meta-material consists of $M = 5$ unit cells. The conclusion from this figure is that the width of the band-gap is decreased along with the selected frequency f_L which was expected. For $f_L < 100[Hz]$, the band-gap width becomes very narrow, but still offers considerable attenuation at the resonant frequencies.

3.2. Structural Realization of a Negative Stiffness Element

In structural mechanics, negative stiffness is generally obtainable through post-buckling processes (snap-through phenomenon). In this case, a single Belleville spring is

Document downloaded by @DAEL, 2026-11-09 07:58:54 - personal use only

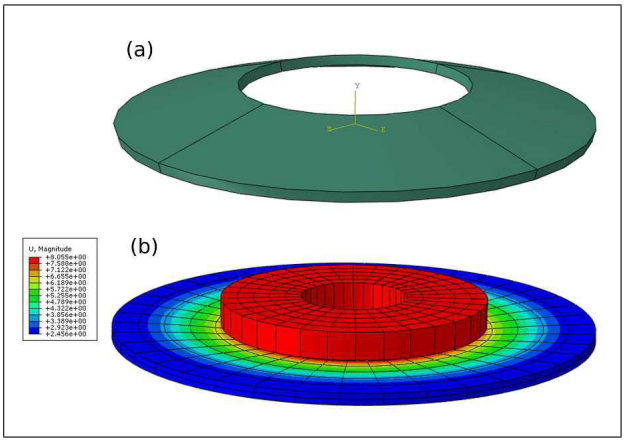


Figure 8. (Colour online) (a) Structural realization of the negative stiffness element k_N, using a Belleville spring. (b) Belleville spring, stressed to the position of zero exerted force.

chosen to act as the negative stiffness element of the oscillator. The exerted force and the equivalent stiffness of this type of springs, are non-linear functions of the vertical displacement s of the inner diameter D_i. The height of the spring is denoted by l_0, D_e is the external diameter and $h_0 \approx l_0 - t$, where t is the thickness. More specific informations are provided by manufacturers [27]. As demonstrated in Figures 9 and 10, the range of the vertical displacement s corresponding to the snap-through region, exhibits the desired negative stiffness characteristics. This of course, translates to the application of a certain pre-stress condition on the spring, so that its stiffness falls in the negative stiffness region, at the equilibrium state of the oscillator.

Figure 8.a shows the shape of the spring, while Figure 8.b presents the deformed spring at the position of zero exerted force ($F = 0$) when appropriate force is applied. In this case, the 2^{nd} part visible in Figure 8.b, is a tool used to uniformly apply the required force. The presented FEM simulation was accomplished via the Arc Length Method, or also commonly called "The modified Riks method" [28, 29]. This method is a powerful numerical technique for solving systems of highly non-linear equations rendering it appropriate for problems that exhibit instabilities, as in this case in the form of buckling. Furthermore, Figure 9 shows a comparison between the results of the analytical and FE methods.

Figure 10 shows the equivalent stiffness of the spring as a function of the vertical displacement s. The dotted orange line, indicates the mean value of k_N in the negative stiffness region, which corresponds to the k_N value used in the linear models, on which the dimensioning of the Belleville spring is based.

3.3. Response to Noise Excitation

3.3.1. Non-Linear Negative Stiffness - Pure Tone Sound Absorption

Initially, in order to investigate the general dynamic behaviour of the meta-material and the effect of the non-linear negative stiffness element as realized via the

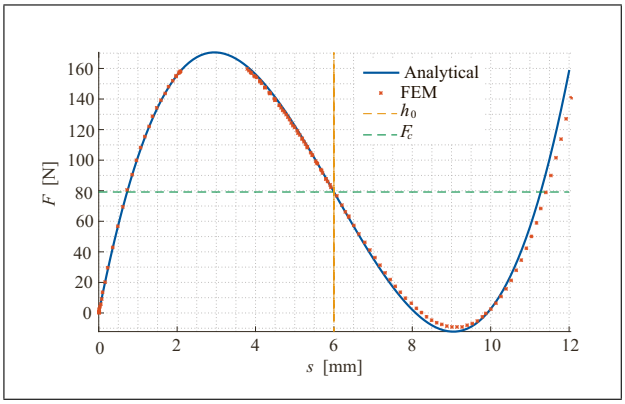


Figure 9. Exerted force of the Belleville spring, as a function of the vertical displacement of its inner diameter.

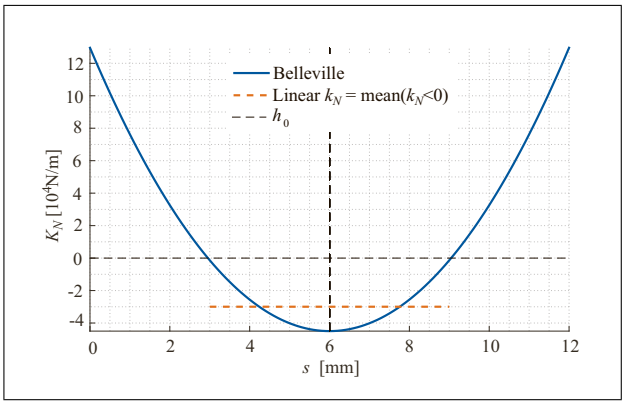


Figure 10. Equivalent stiffness of the Belleville spring, as a function of the vertical displacement of its inner diameter.

Belleville spring, a harmonic excitation is applied, considering an incident plane wave on the surface of the 1st mass, with frequency $f = f_L = 200$ [Hz]. The surface in question is considered as a 0.1×0.1 [m] rectangle, therefore the area is $A = 0.01$ [m^2]. Consequently, the excitation force comes as

$$F(t) = F_0 e^{j2\pi f_L t}, \tag{83}$$

where

$$F_0 = \hat{p}A, \hat{p} = \frac{2}{\sqrt{2}} p_{ref} 10^{L_p/20}, \tag{84}$$

and $L_p = 100$ [dB] is the considered sound pressure level. This level of noise is chosen in order to simulate the response of the meta-material under extreme noise conditions. Observation of Figure 11, does not show any significant deviations between the linear and non-linear negative stiffness simulations. Besides, it is obvious that the magnitude of the resulting displacements of the oscillators, is orders of magnitude lower than the required to introduce any significant non-linearity via the Belleville springs.

The required, initial, vertical displacement s of the Belleville springs (pre-stress), comes from the static equilibrium equations of the unit cell. Figure 12 shows the time history of $k_{N,1}$ to $k_{N,M=5}$ values, along with the linear k_N stiffness, denoted by the green dotted line. Namely,

Document downloaded by @DAEL, 2026-11-09 07:58:54 - personal use only

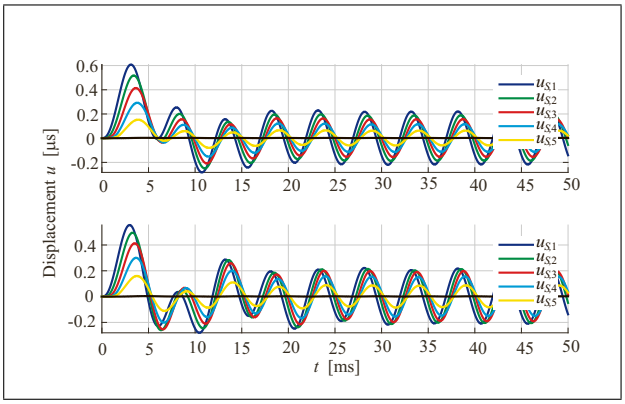


Figure 11. (Colour online) Time response of KDamper meta-material with $M = 5$ unit cells to harmonic excitation with frequency $f = f_L = 200$ [Hz].

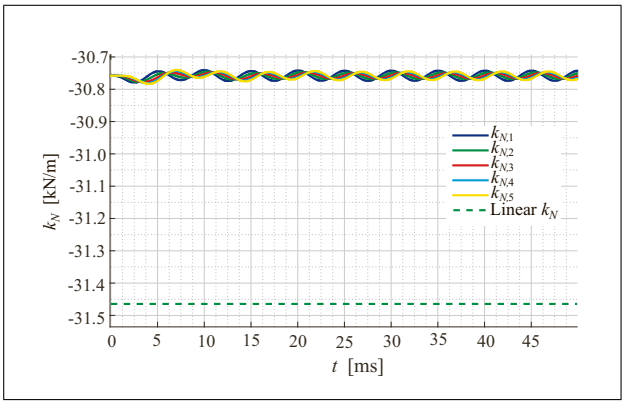


Figure 12. (Colour online) Time response of the non-linear stiffness of the negative stiffness elements realized with Belleville springs, for a KDamper meta-material with $M = 5$ unit cells. Comparison with linear k_N.

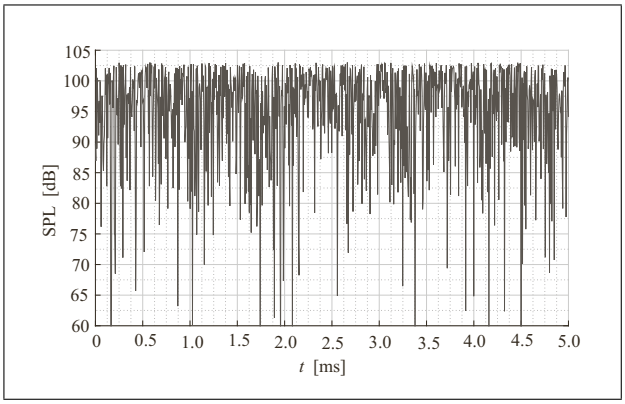


Figure 13. SPL sample of the random broadband noise, with frequencies $f_n \epsilon$ [200 : 400] [Hz], used as excitation of the meta-material.

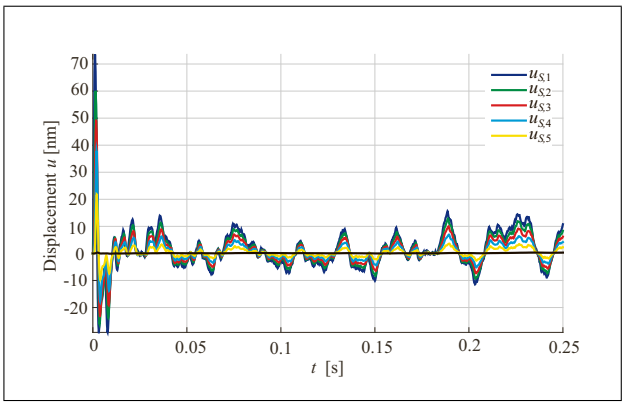


Figure 14. (Colour online) Time response of KDamper meta-material with $M = 5$ unit cells to random broadband noise with frequencies $f_n \epsilon$ [200 : 400] [Hz].

the $k_{N,i}$ values of the Belleville springs, oscillate around the corresponding stiffness value of the aforementioned equilibrium position, which is approximating the linear k_N value.

3.3.2. Broadband Noise Absorption

In order to further examine the behaviour of the KDamper meta-material, a case of random noise acting as the excitation is considered. The content of this noise, is composed by a number of plane waves at frequencies between 200 and 400 Hz with random phase angles and amplitudes. Specifically, these features are generated as follows:

$$f_i = f_L\,(N(0,1)+1), \tag{85}$$

$$\mathbf{F} = \sum_{i=1}^{h} |C_i| e^{j2\pi f_i t}, \tag{86}$$

where

$$C_i = \alpha_0 e^{j\phi}, \tag{87}$$

$$\alpha_0 = F_0\,N(0,1), \quad \phi = N(0,1), \tag{88}$$

and $N(0,1)$ are random numbers from a Gaussian distribution with zero mean and variance equal to unity. The resulting sound pressure level is displayed in Figure 13.

Considering a KDamper meta-material with M=5 unit cells, the response is presented in Figure 14. The displacements of the added masses ($u_{D,1}, u_{D,2}$... etc.),are excluded, in order to have a clearer picture.

From Figure 14, comparing the displacement $u_{S,1}$ of the 1st mass to $u_{S,5}$ of the last mass, the expected attenuation is present here as indicated by T_{KD} in Figure 6 and also observed in Figure 11 for the case of harmonic excitation, despite the broadband nature of the excitation.

3.4. Comparison of "m-k-m", TMD and KDamper Based Acoustic Metamaterials

A conventional "sandwich type" noise isolation panel, consisting of two plates with a noise insulation material between them and can be considered as a simple mass-spring-mass ("m-k-m") system, with some degree of internal damping. In view of Figure 4, this corresponds to a system with $M = 1$, $m_D = c_D = k_N = k_P = 0$. Periodic repetition of this lattice results to a primitive form of a "phononic crystal" type of acoustic insulation meta-material. The introduction of an internal structure between the masses in the form of a TMD ($m_D, c_D, k_P \neq 0$) results to an acoustic meta-material design. The additional inclu-

Document downloaded by @DAEL, 2026-11-09 07:58:54 - personal use only

Table II. Values of the basic parameters of the meta-materials.

	μ	ζ	ζ_D
m-k-m	-	0.15	-
TMD	0.5	0.15	0.707
KDamper	0.01	0.15	0.707
	f_L [Hz]	m [kg]	m_D [kg]
m-k-m	-	0.035	-
TMD	200	0.035	$17.5 \cdot 10^{-3}$
KDamper	200	0.035	$0.35 \cdot 10^{-3}$
	k_S [N/m]	k_0 [N/m]	k_P [N/m]
m-k-m	$6.76 \cdot 10^4$	-	-
TMD	$6.76 \cdot 10^4$	-	$2.76 \cdot 10^4$
KDamper	$3.99 \cdot 10^5$	$6.70 \cdot 10^4$	$3.48 \cdot 10^4$
	k_N [N/m]	c_S [Ns/m]	c_D [Ns/m]
m-k-m	-	14.59	-
TMD	-	-	31.10
KDamper	$-3.15 \cdot 10^4$	14.53	1.52

sion of a negative stiffness element ($k_N \neq 0$), results to a KDamper based meta-material.

The isolation-absorption properties of these three alternative concepts are compared here. The various meta-structures implemented have relevant unit lattice parameters summarized on Table 2 along with the resulting corresponding stiffness and damping elements in each case. The selection of the parameters ensures that all three unit lattice types have the same overall static stiffness. For this last reason, the overall static stiffness k_S of the periodic mass-spring-mass system is the same as the static stiffness of the TMD based meta-material. However, in view of Equation (1), the value of k_S has to be increased for the KDamper meta-material, so that its overall static stiffness (now k_0) is equal to the overall static stiffness k_S of the other two types. Finally, the parameter κ of the KDamper meta-material is selected as $0.9\kappa_{\max}$.

The comparisons between the three different concepts on the transfer function of the system are presented in Figures 15-17. The "m-k-m" system essentially acts as a low pass filter for the noise with a cutoff frequency of $f_0 = 442.33[Hz]$. Observation of Figures 15-17 indicates that the repetition of unit cells does not improve the low pass behavior. It just increases the high frequency filtering capability of this system. This behaviour is typical of the current noise isolation panels.

The TMD based meta-material retains this low pass filter behavior, while introducing a deep but very narrow band gap. The width of this band-gap is approximately [200 [Hz]:245 [Hz]]. However, in order to achieve this band-gap, an additional mass of 50% of the original mass of the meta-material is required. The repetition of unit cells does not improve the low pass behaviour or the band-gap boundaries. It just increases the high frequency filtering

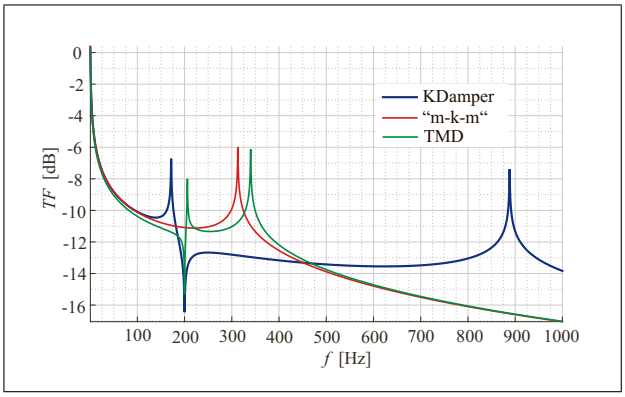


Figure 15. (Colour online) Comparison of the transfer functions of the three acoustic isolation-absorption systems for $M = 1$, $f_L = f_D = 200$ [Hz].

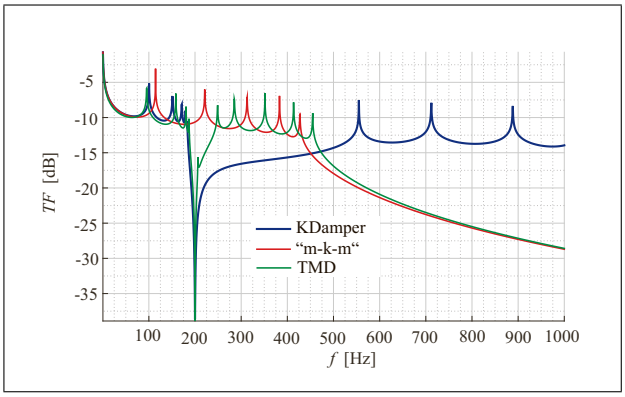


Figure 16. (Colour online) Comparison of the transfer functions of the three acoustic isolation-absorption systems for $M = 5$, $f_L = f_D = 200$ [Hz].

capability of this system, as well as the depth of the band-gap.

The KDamper meta-material essentially operates as a band-stop filter. Although its high frequency behaviour is less satisfactory than the periodic "m-k-m" system and the TMD based meta-material, it is very effective in introducing a very wide band gap of a [200Hz:490Hz] width while incorporating an added mass of only 1% of the value of the mass m. The repetition of unit cells, as presented in Figure 5 increases the depth of the band-gap, while bearing a marginal effect on the high frequency behaviour of the system.

4. Conclusion

Although acoustic meta-materials have been long considered to present the only available direction to create band-gaps at wavelengths much longer than the lattice size, and thus enable low-frequency vibration attenuation, the width of the resulting band gaps is generally very narrow –especially when referring to the conventional "m-k-m" and TMD based periodic structures considered in the presented comparisons– since it depends on the ratio of the internal oscillating mass to the external mass of the unit

Document downloaded by @DAEL, 2026-11-09 07:58:54 - personal use only

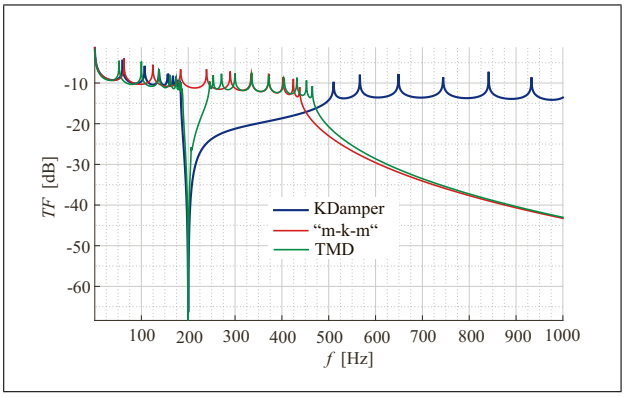


Figure 17. (Colour online) Comparison of the transfer functions of the three acoustic isolation-absorption systems for $M = 10$, $f_L = f_D = 200$ [Hz].

lattice. Meta-materials based on the KDamper concept can overcome this disadvantage, since they exploit the additional synergy of a negative stiffness element inclusion. Thus, they prove highly efficient in generating wide band-gaps in low frequency applications, with only a small fraction of the external mass. Appropriate technological implementations of this concept can lead to drastic improvements in all types of low-frequency technological applications, with emphasis in low-frequency noise isolation-absorption. Future research objectives regarding this concept, include further examination of the meta-material response to broadband low frequency noise, involving computational simulations and experimental tests of practical implementations like panels, for determination of properties such as Transmission Loss and sound reflection among others.

Acknowledgement

This work was supported in part by the European Cooperation in Science and Technology (COST) action DENORMS (Designs for Noise Reducing Materials and Structures) – CA 15125, within the Horizon 2020 Framework Programme of the European Union.

References

[1] M. I. Hussein, M. J. Leamy, M. Ruzzene: Dynamics of phononic materials and structures: Historical origins, recent progress and future outlook. Applied Mechanics Reviews **66** (2014) 040802–040802–040838.

[2] M. M. Sigalas, E. N. Economou: Elastic and acoustic wave band structure. Journal of Sound and Vibration **158** (1992) 377–382.

[3] J. O. Vasseur, B. Djafari-Rouhani, L. Dobrzynski, M. S. Kushwaha, P. Halevi: Complete acoustic band gaps in periodic fibre reinforced composite materials: the carbon/epoxy composite and some metallic systems. Journal of Physics: Condensed Matter **6** (1994) 8759.

[4] Z. Liu, X. Zhang, Y. Mao, Y. Y. Zhu, Z. Yang, C. T. Chan, et al.: Locally resonant sonic materials. Science **289** (2000) 1734–1736.

[5] H. Huang, C. Sun, G. Huang: On the negative effective mass density in acoustic metamaterials. International Journal of Engineering Science **47** (2009) 610–617.

[6] J. L. Auriault, G. Bonnet: Dynamique des composites elastiques periodiques. Arch. Mech. **37** (1985) 269–284.

[7] J. L. Auriault: Acoustics of heterogeneous media: Macroscopic behavior by homogenization. Current Topics in Acoust. Res. **1** (1994) 63–90.

[8] H. Sun, X. Du, P. F. Pai: Theory of metamaterial beams for broadband vibration absorption. Journal of Intelligent Material Systems and Structures **21** (2010) 1085–1101.

[9] Y. Xiao, J. Wen, D. Yu, X. Wen: Flexural wave propagation in beams with periodically attached vibration absorbers: Band-gap behavior and band formation mechanisms. Journal of Sound and Vibration **332** (2013) 867–893.

[10] Y. Pennec, B. Djafari-Rouhani, H. Larabi, J. O. Vasseur, A. C. Hladky-Hennion: Low-frequency gaps in a phononic crystal constituted of cylindrical dots deposited on a thin homogeneous plate. Physical Review B **78** (2008) 104105.

[11] H. Peng, P. Frank Pai: Acoustic metamaterial plates for elastic wave absorption and structural vibration suppression. International Journal of Mechanical Sciences **89** (2014) 350–361.

[12] J. P. Groby, C. Lagarrigue, B. Brouard, O. Dazel, V. Tournat, B. Nennig: Using simple shape three-dimensional rigid inclusions to enhance porous layer absorption. Journal of the Acoustical Society of America **136** (2014) 1139–1148.

[13] T. Weisser, L. Schwan, J. P. Groby, C. Lagarrigue, E. Deckers, O. Dazel: Poroelastic subwavelength absorber with both elastic and acoustic embedded resonator. Proceedings of the 27th International Conference on Noise and Vibration Engineering, 2016, 2127–2136.

[14] Z. Yang, H. M. Dai, N. H. Chan, G. C. Ma, P. Sheng: Acoustic metamaterial panels for sound attenuation in the 50–1000 Hz regime. Applied Physics Letters **96** (2010) 041906.

[15] L. Schwan, O. Umnova, C. Boutin: Sound absorption and reflection from a resonant metasurface: Homogenisation model with experimental validation. Wave Motion **72** (2017) 154–172.

[16] I. Antoniadis, D. Chronopoulos, V. Spitas, D. Koulocheris: Hyper-damping properties of a stable linear oscillator with a negative stiffness element. Journal of Sound and Vibration **346** (2015) 37–52.

[17] I. A. Antoniadis, S. A. Kanarachos, K. Gryllias, I. E. Sapountzakis: Kdamping: A stiffness based vibration absorption concept. Journal of Vibration and Control **24** (2016) 588–606.

[18] D. Chronopoulos, I. Antoniadis, T. Ampatzidis: Enhanced acoustic insulation properties of composite metamaterials having embedded negative stiffness inclusions. Extreme Mechanics Letters **12** (2017) 48–54.

[19] D. Chronopoulos, I. Antoniadis, M. Collet, M. Ichchou: Enhancement of wave damping within metamaterials having embedded negative stiffness inclusions. Wave Motion **58** (2015) 165–179.

[20] P. Michelis, V. Spitas: Numerical and experimental analysis of a triangular auxetic core made of CFR-PEEK using the Directionally Reinforced Integrated Single-yarn (DIRIS) architecture. Composites Science and Technology **70** (2010) 1064–1071.

[21] K. Virk, A. Monti, T. Trehard, M. Marsh, K. Hazra, K. Boba, et al.: SILICOMB PEEK Kirigami cellular structures: mechanical response and energy dissipation through zero and negative stiffness. Smart Materials and Structures **22** (2013) 084014.

Document downloaded by @DAEL, 2026-11-09 07:58:54 - personal use only

[22] E. Baravelli, M. Ruzzene: Internally resonating lattices for bandgap generation and low-frequency vibration control. Journal of Sound and Vibration **332** (2013) 6562–6579.

[23] P. Wang, F. Casadei, S. Shan, J. C. Weaver, K. Bertoldi: Harnessing buckling to design tunable locally resonant acoustic metamaterials. Physical Review Letters **113** (2014) 014301.

[24] M. I. Hussein, M. J. Frazier: Metadamping: An emergent phenomenon in dissipative metamaterials. Journal of Sound and Vibration **332** (2013) 4767–4774.

[25] H. H. Huang, C. T. Sun: Wave attenuation mechanism in an acoustic metamaterial with negative effective mass density. New Journal of Physics **11** (2009) 013003.

[26] C. Sugino, S. Leadenham, M. Ruzzene, A. Erturk: On the mechanism of bandgap formation in locally resonant finite elastic metamaterials. Journal of Applied Physics **120** (2016) 134501.

[27] C. Bauer: Disc springs-theory and practice. Retrieved from https://www.christianbauer.com/en/img-cust/3_Theory_and_practice.pdf, March 29, 2008.

[28] E. Riks: An incremental approach to the solution of snapping and buckling problems. International Journal of Solids and Structures **15** (1979) 529–551.

[29] M. Crisfield: A fast incremental/iterative solution procedure that handles "snap-through". Computational Methods in Nonlinear Structural and Solid Mechanics (1981) 55–62.

Document downloaded by @DAEL, 2026-11-09 07:58:54 - personal use only